Chapter 12
Modelling in Applied Fluid Dynamics

This chapter differs substantially from the previous chapters in that we do not aim to explain any new methodologies here. Instead, we will make use the approaches developed earlier to illustrate two case studies of how mathematical models of physical problems can be formulated and analysed.

Our two examples applications come from problems in fluid dynamics, on air bearing sliders and wedge-rivulet flow. We begin by deriving a common core-model, called *lubrication theory*, that forms the basis for both applications. While the derivation of lubrication theory draws extensively on the methods for long-wave asymptotics that were introduced in Chap. 8, we will not attempt to individually identify the many other connections between the material in this chapter and the methods given in the other earlier chapters. Having this background, readers should be comfortable with the presentations here, which are at levels that are typical of basic modelling in current applied research and case studies in more advanced books on modelling [27, 37, 96]. For further examples of case studies in mathematical modelling see [51, 53, 69].

12.1 Lubrication Theory

The Navier-Stokes equations comprise the fundamental continuum mechanics mathematical model for the dynamics of fluids having viscosity (namely, realistic dissipation or internal friction). These partial differential equations are conservation laws for mass and momentum of fluids and universally applicable. However, for a number of analytical and computational reasons, they can be very challenging to solve for most problems. Consequently, to make progress, most applied studies make use of specific forms of their problems to further reduce the Navier-Stokes equations to more tractable models. For problems that involve slender layers of viscous fluids, *lubrication models* can be derived from the Navier-Stokes equations using asymptotics in terms of the dominance of viscous effects and the slenderness of the layer. Dat-

T. Witelski and M. Bowen, *Methods of Mathematical Modelling*,
Springer Undergraduate Mathematics Series, DOI 10.1007/978-3-319-23042-9_12

ing back to the work of Osborne Reynolds (1842–1912), such models have become essential for advancing the analysis of problems from a diverse range of applications.

We begin with the Navier-Stokes equations for a compressible viscous Newtonian fluid. Written in vector form, the continuity equation and momentum balance are

$$\frac{\partial \tilde{\rho}}{\partial \mathsf{T}} + \nabla \cdot (\tilde{\rho}\mathbf{V}) = 0, \qquad \tilde{\rho}\left(\frac{\partial \mathbf{V}}{\partial \mathsf{T}} + \mathbf{V} \cdot \nabla \mathbf{V}\right) = -\nabla \mathsf{P} + \mu \nabla^2 \mathbf{V}, \tag{12.1}$$

where μ is the viscosity coefficient, $\tilde{\rho}(\mathsf{X}, \mathsf{Y}, \mathsf{Z}, \mathsf{T})$ is the fluid density, $\mathsf{P}(\mathsf{X}, \mathsf{Y}, \mathsf{Z}, \mathsf{T})$ is the pressure, and the fluid velocity field is $\mathbf{V}(\mathsf{X}, \mathsf{Y}, \mathsf{Z}, \mathsf{T}) = (\mathsf{U}, \mathsf{V}, \mathsf{W})$. Expanded out componentwise (12.1) yields a system of four coupled nonlinear PDEs,

$$\tilde{\rho}_{\mathsf{T}} + (\tilde{\rho}\mathsf{U})_{\mathsf{X}} + (\tilde{\rho}\mathsf{V})_{\mathsf{Y}} + (\tilde{\rho}\mathsf{W})_{\mathsf{Z}} = 0, \tag{12.2a}$$

$$\tilde{\rho}(\mathsf{U}_{\mathsf{T}} + \mathsf{U}\mathsf{U}_{\mathsf{X}} + \mathsf{V}\mathsf{U}_{\mathsf{Y}} + \mathsf{W}\mathsf{U}_{\mathsf{Z}}) = -\mathsf{P}_{\mathsf{X}} + \mu(\mathsf{U}_{XX} + \mathsf{U}_{YY} + \mathsf{U}_{ZZ}), \tag{12.2b}$$

$$\tilde{\rho}(\mathsf{V}_{\mathsf{T}} + \mathsf{U}\mathsf{V}_{\mathsf{X}} + \mathsf{V}\mathsf{V}_{\mathsf{Y}} + \mathsf{W}\mathsf{V}_{\mathsf{Z}}) = -\mathsf{P}_{\mathsf{Y}} + \mu(\mathsf{V}_{XX} + \mathsf{V}_{YY} + \mathsf{V}_{ZZ}), \tag{12.2c}$$

$$\tilde{\rho}(\mathsf{W}_{\mathsf{T}} + \mathsf{U}\mathsf{W}_{\mathsf{X}} + \mathsf{V}\mathsf{W}_{\mathsf{Y}} + \mathsf{W}\mathsf{W}_{\mathsf{Z}}) = -\mathsf{P}_{\mathsf{Z}} + \mu(\mathsf{W}_{XX} + \mathsf{W}_{YY} + \mathsf{W}_{ZZ}). \tag{12.2d}$$

For convenience, we simplify our presentation to the two-dimensional problem[1] where $\mathsf{W} \equiv 0$ and all properties are independent of Z (i.e. $\partial_{\mathsf{Z}} \equiv 0$) and hence consider the system,

$$\tilde{\rho}_{\mathsf{T}} + (\tilde{\rho}\mathsf{U})_{\mathsf{X}} + (\tilde{\rho}\mathsf{V})_{\mathsf{Y}} = 0, \tag{12.3a}$$

$$\tilde{\rho}(\mathsf{U}_{\mathsf{T}} + \mathsf{U}\mathsf{U}_{\mathsf{X}} + \mathsf{V}\mathsf{U}_{\mathsf{Y}}) = -\mathsf{P}_{\mathsf{X}} + \mu(\mathsf{U}_{XX} + \mathsf{U}_{YY}), \tag{12.3b}$$

$$\tilde{\rho}(\mathsf{V}_{\mathsf{T}} + \mathsf{U}\mathsf{V}_{\mathsf{X}} + \mathsf{V}\mathsf{V}_{\mathsf{Y}}) = -\mathsf{P}_{\mathsf{Y}} + \mu(\mathsf{V}_{XX} + \mathsf{V}_{YY}). \tag{12.3c}$$

We consider the dynamics of a thin layer of viscous fluid spreading on a flat solid surface, as shown in Fig. 12.1, with the average height given by $\bar{\mathrm{H}}$ and the lateral lengthscale given by $\bar{\mathrm{L}}$. We formally nondimensionalize using the scalings

$$\mathsf{X} = \bar{\mathrm{L}}x, \qquad \mathsf{Y} = \bar{\mathrm{H}}y, \qquad \mathsf{T} = \bar{\mathrm{T}}t, \tag{12.4a}$$

$$\mathsf{U} = \bar{\mathrm{U}}u, \qquad \mathsf{V} = \bar{\mathrm{V}}v, \qquad \mathsf{P} = \bar{\mathrm{P}}p, \qquad \tilde{\rho} = \bar{\rho}\rho. \tag{12.4b}$$

We go on to use the aspect ratio $\varepsilon = \mathrm{H}/\mathrm{L}$ as an asymptotic parameter, $\varepsilon \to 0$.

Applying the scalings to (12.3a) yields the nondimensional form

$$\frac{\partial \rho}{\partial t} + \left(\frac{\bar{\mathrm{U}}\bar{\mathrm{T}}}{\bar{\mathrm{L}}}\right)\frac{\partial}{\partial x}(\rho u) + \left(\frac{\bar{\mathrm{V}}\bar{\mathrm{T}}}{\bar{\mathrm{H}}}\right)\frac{\partial}{\partial y}(\rho v) = 0.$$

Conservation of mass is a fundamental property and it should hold exactly, independent of the geometry or any considerations of flow speed. Hence, independent of the final choice of characteristic scales, we should retain the general form given

[1] The derivation for the full three-dimensional system follows analogously.

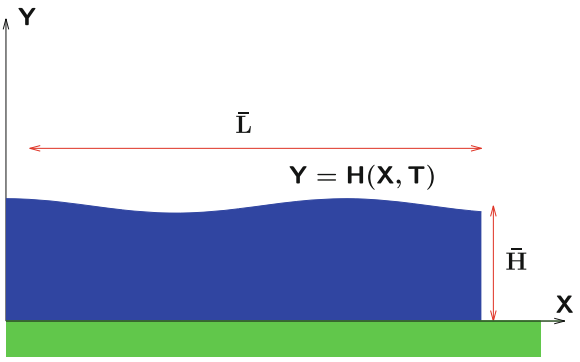

Fig. 12.1 A thin film of a viscous fluid coating a flat solid surface

by (12.3a). This motivates selecting scales to make the continuity equation scale-invariant; namely we pick a convective timescale $T = L/U$ and a vertical velocity scale based on the horizontal velocity and the aspect ratio, $V = \varepsilon U$, to yield the final dimensionless equation,

$$\frac{\partial \rho}{\partial t} + \frac{\partial}{\partial x}(\rho u) + \frac{\partial}{\partial y}(\rho v) = 0. \tag{12.5}$$

Turning to the momentum equations, using the scalings, the non-dimensional forms of (12.3b, 12.3c) are

$$\left(\varepsilon^2 \frac{\bar{\rho}\bar{U}\bar{L}}{\mu}\right)(u_t + uu_x + vu_y) = -\left(\varepsilon^2 \frac{\bar{P}\bar{L}}{\mu\bar{U}}\right) p_x + \varepsilon^2 u_{xx} + u_{yy}, \tag{12.6a}$$

$$\left(\varepsilon^2 \frac{\bar{\rho}\bar{U}\bar{L}}{\mu}\right)(v_t + uv_x + vv_y) = -\left(\frac{\bar{P}\bar{L}}{\mu\bar{U}}\right) p_y + \varepsilon^2 v_{xx} + v_{yy}. \tag{12.6b}$$

Apart from the aspect ratio, these equations contain two dimensionless parameters. The reduced Reynolds number gives the ratio of effects of inertial acceleration relative to viscous forces,

$$\widetilde{\mathrm{Re}} = \varepsilon^2 \frac{\bar{\rho}\bar{U}\bar{L}}{\mu} \ll 1, \tag{12.7}$$

To assert the dominance of viscous effects, we assume that this parameter is negligibly small.
Consequently, (12.6a, 12.6b) reduces to

$$0 = -\left(\varepsilon^2 \frac{\bar{P}\bar{L}}{\mu\bar{U}}\right) p_x + \varepsilon^2 u_{xx} + u_{yy}, \tag{12.8a}$$

$$0 = -\left(\frac{\bar{P}\bar{L}}{\mu\bar{U}}\right) p_y + \varepsilon^2 v_{xx} + v_{yy}. \tag{12.8b}$$

We note that this reduction of the Navier Stokes equations (having removed the nonlinear inertial acceleration terms) is called the *Stokes equations*, and for the incompressible (constant density) case, their dimensional form is

$$\mathbf{0} = -\nabla \mathsf{P} + \mu \nabla^2 \mathbf{V}, \qquad \nabla \cdot \mathbf{V} = 0. \tag{12.9}$$

The choice of the pressure scaling in (12.8a, 12.8b) remains. One option is to apply dominant balance to the y-momentum equation, yielding the derived scale $\bar{\mathsf{P}} = \mu \bar{\mathrm{U}}/\bar{\mathrm{L}} = O(1)$, which is called a viscous pressure scale since it balances viscous and pressure-gradient effects. However it can be shown from the resulting leading order x-equation, $u_{0yy} = 0$, that for many problems, this choice can be too restrictive and may to lead to solutions that will not capture the full structure of the flow. The other option is dominant balance in the x-equation, yielding another version of the viscous pressure scale, $\bar{\mathsf{P}} = \mu \bar{\mathrm{U}}/(\varepsilon^2 \bar{\mathrm{L}}) = O(\varepsilon^{-2})$. This leads to the leading order system,

$$\frac{\partial p_0}{\partial x} = \frac{\partial^2 u_0}{\partial y^2}, \qquad \frac{\partial p_0}{\partial y} = 0. \tag{12.10}$$

The second equation determines that p_0 is independent of y, namely $p_0 = p_0(x, t)$. Consequently the first equation can be integrated with respect to y to yield a parabolic form, sometimes called the *Nusselt velocity profile*,

$$u_0 = \tfrac{1}{2} \frac{\partial p_0}{\partial x} y^2 + C_1 y + C_2, \tag{12.11}$$

where C_1, C_2 are constants of integration with respect to y. These constants are determined by boundary conditions on the lateral velocity u at the top and bottom of the fluid layer for the particular problem at hand.

For viscous fluids in contact with solids, the *no-slip boundary condition* states that the velocity of the fluid tangential to the solid must match that of the solid. In this problem the solid surface is $y = 0$, and the no-slip condition specifies that $u_0(0) = 0$, which determines $C_2 = 0$ in (12.11). At the surface of the layer, $y = h(x, t)$, if the fluid were not subjected to any forces (surface stresses) then the lateral speed at the surface should be the same as the bulk of the fluid; the simplest form of the *stress-free boundary condition* is then

$$\left. \frac{du_0}{dy} \right|_{y=h} = 0 \qquad \Longrightarrow \qquad C_1 = -p_{0x}(x, t) h(x, t). \tag{12.12}$$

Consequently, we have determined that for films spreading on flat surfaces,

$$u_0(x, y, t) = \tfrac{1}{2} p_{0x} (y^2 - 2hy). \tag{12.13}$$

To complete the derivation of the lubrication model, we return to the equation for the conservation of mass, (12.5), and integrate it over the thickness of the layer,

$$\int_0^h \left[\frac{\partial \rho}{\partial t} + \frac{\partial}{\partial x}(\rho u) + \frac{\partial}{\partial y}(\rho v) \right] dy = 0.$$

The final term can be integrated directly to give a relation between the fluxes through the bottom and top of the layer,

$$\rho v \Big|_{y=0}^{y=h} = -\int_0^h \left[\frac{\partial \rho}{\partial t} + \frac{\partial}{\partial x}(\rho u) \right] dy. \tag{12.14}$$

At $y = 0$, the fluid rests on an impermeable solid surface, so there should be no flux through it, hence the no-flux boundary condition gives $v(y = 0) = 0$. At the top of the layer, the fluid has a free boundary, and the vertical component of the velocity there should follow the motion of the surface $y = h(x, t)$. Consider a particle on the surface that is carried by the flow, having position $(X(t), Y(t))$, and remains on the surface for all times, so $Y(t) = h(X(t), t)$. Then, using the chain rule and recalling the Lagrangian description of the velocity, the rate of change of the vertical position of any point on a free boundary is given by

$$\frac{dY}{dt} = \frac{\partial h}{\partial t} + \frac{\partial h}{\partial x}\frac{dX}{dt} \qquad \Longrightarrow \qquad v\Big|_{y=h} = \frac{\partial h}{\partial t} + u\frac{\partial h}{\partial x}\Big|_{y=h}, \tag{12.15}$$

which is called the *kinematic boundary condition*. Applying these two boundary conditions to (12.14) yields

$$\left(\rho \frac{\partial h}{\partial t} + \rho u \frac{\partial h}{\partial x} \right) \Big|_{y=h} + \int_0^h \left[\frac{\partial \rho}{\partial t} + \frac{\partial}{\partial x}(\rho u) \right] dy = 0.$$

Applying Leibniz's rule (in reverse, with respect to x and t separately) then gives a transport equation describing conservation of mass

$$\frac{\partial}{\partial t}\left(\int_0^h \rho \, dy \right) + \frac{\partial}{\partial x}\left(\int_0^h \rho u \, dy \right) = 0. \tag{12.16}$$

If we take $\rho = \rho(x, t)$ then this reduces to

$$\frac{\partial (\rho h)}{\partial t} + \frac{\partial}{\partial x}\left(\rho \int_0^h u \, dy \right) = 0. \tag{12.17}$$

Finally, using the velocity profile (12.13) to evaluate the integral yields

$$\frac{\partial(\rho h)}{\partial t} = \frac{1}{3}\frac{\partial}{\partial x}\left(\rho h^3 \frac{\partial p}{\partial x}\right). \tag{12.18}$$

This is a form of the *Reynolds equation* that forms the basis of lubrication models in a wide array of applications involving free-surface thin film flows [25, 75, 79, 82] and fluid-structure interactions involving lubricating fluid layers [12, 46].

12.2 Dynamics of an Air Bearing Slider

One of the historical motivations for the development of lubrication theory has been the use of fluids as cushioning layers between moving surfaces—an everyday application is oil lubricating parts of an engine to allow relative motion without metal surfaces scratching against each other.

Lubrication theory is also used in modern technology [12]—in computer hard disk drives, air acts as a lubricating gas layer separating the electronic read/write head from the rapidly rotating rigid data disks. To maximize the data density on the disk, the write head must be kept very close to the surface, and to maximize data access speed, the disk speed should be high. However both of these effects might suggest the system could be sensitive to any variations in disk speed, external forces and motion of the system, or variations of pressure that might lead the head to collide with the disk. Hence it is very important to have a model of the system that can guide the design process to configurations that are stable to perturbations.

The one-dimensional[2] version of the geometry we are considering is shown in Fig. 12.2. The read/write head, sometimes also called a *slider bearing* [79], has a particular length $\bar{\mathrm{L}}$ and has its lateral position fixed, but it is allowed to move vertically. The disk is a flat surface ($\mathsf{Y} = 0$) moving horizontally at local speed $\bar{\mathrm{U}}$. The motion of the disk will generate a flow of air under the slider due to the no-slip boundary condition on the gas. This flow will generate a lift force on the slider that will balance against the weight of the slider and any other applied downward forces. The desired average gap height $\bar{\mathrm{H}}$ sets a vertical lengthscale. The gap height between the disk and slider surfaces is given by

$$\mathsf{H}(\mathsf{X}, \mathsf{T}) = \mathsf{A}(\mathsf{T}) + \mathsf{S}(\mathsf{X}), \tag{12.19}$$

where A is the vertical position of the leading edge of the slider and $\mathsf{S}(\mathsf{X})$ gives the shape of the slider's lower surface, with $\mathsf{S}(0) = 0$. Outside of the region under the slider, the air pressure will be assumed to be the usual atmospheric pressure, $\mathrm{P}_{\mathrm{atm}}$.

[2] Referring to the number of lateral dimensions.

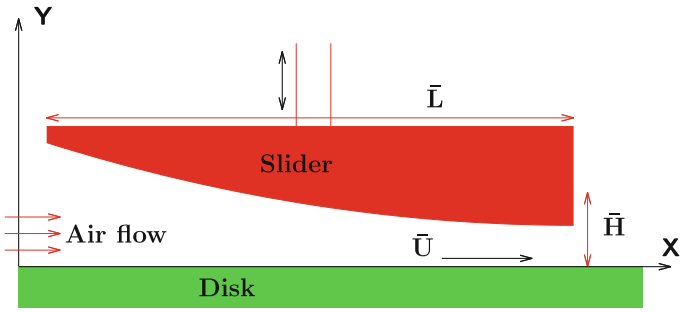

Fig. 12.2 The geometry of the problem for an air bearing slider. Lubrication theory can be applied to model the air flow in the thin gap between the moving disk and slider surfaces

Under the assumption that the reduced Reynolds number is small, (12.7), and that the aspect ratio of the gap is small, $\varepsilon \equiv \bar{H}/\bar{L} \ll 1$, lubrication theory can be applied. Written in dimensional form, the parabolic velocity profile (12.11) in the gap is

$$U = \frac{1}{2\mu}\frac{\partial P}{\partial X}Y^2 + C_1 Y + C_2. \tag{12.20}$$

The scalings and boundary conditions appropriate to this problem must be applied to this general form. At the disk and slider surfaces, no-slip boundary conditions impose the lateral speeds on the gas flow,

$$U(Y = 0) = \bar{U}, \qquad U(Y = H) = 0.$$

These conditions select the constants of integration in (12.20) to yield

$$U = \frac{1}{2\mu}\frac{\partial P}{\partial X}(Y^2 - HY) + \bar{U}\left(1 - \frac{Y}{H}\right), \tag{12.21}$$

where we have separated the contributions due to the pressure-gradient driven Poiseuille flow term and the linear shear-flow Couette flow term. The next step is to use this velocity profile in the equation of conservation of mass to derive the appropriate form of the Reynolds equation for this problem.

While Eq. (12.16) was derived under a different type of boundary condition on the upper surface of the fluid layer, it can be shown that the same equation is obtained when the kinematic boundary condition is replaced by a no-flux condition appropriate to the interface with the slider surface at $Y = H$ [46]. This could be expected from physical considerations of (12.17) as a transport equation; since the mass of air in any column, $\tilde{\rho}H$, is conserved, its rate of change can only be due to transport to other positions in the gap by the flux. Consequently, we obtain the dimensional equation

$$\frac{\partial(\tilde{\rho}H)}{\partial T} + \frac{\bar{U}}{2}\frac{\partial(\tilde{\rho}H)}{\partial X} = \frac{1}{12\mu}\frac{\partial}{\partial X}\left(\tilde{\rho}H^3\frac{\partial P}{\partial X}\right). \tag{12.22}$$

To nondimensionalize this equation, we need to select characteristic scales. For the velocity scale, it is natural to use the imposed disk speed $\bar{\mathrm{U}}$. For the lateral length scale, the length of the slider, $\bar{\mathrm{L}}$, is a convenient choice; the derived convective timescale is then $\bar{\mathrm{T}} = \bar{\mathrm{L}}/\bar{\mathrm{U}}$. In the vertical direction, the reference height $\bar{\mathrm{H}}$ can be used. Equation (12.22) is linear with respect to $\tilde{\rho}$, so whatever the choice of the characteristic density, it will scale out. The boundary conditions on the pressure at the edges of the slider give an imposed pressure scale, $\bar{\mathrm{P}} = \mathrm{P}_{\mathrm{atm}}$. Using these scalings in (12.4) and writing $\mathsf{H} = \bar{\mathrm{H}}h$ we obtain the dimensionless equation [30, 46]

$$\frac{\partial(\rho h)}{\partial t} + \tfrac{1}{2}\frac{\partial(\rho h)}{\partial x} = \frac{1}{\Lambda}\frac{\partial}{\partial x}\left(\rho h^3 \frac{\partial p}{\partial x}\right),$$

containing one dimensionless parameter, called the *bearing number*,

$$\Lambda = \frac{12\mu\bar{\mathrm{L}}\bar{\mathrm{U}}}{\mathrm{P}_{\mathrm{atm}}\bar{\mathrm{H}}^2}, \tag{12.23}$$

which gives the ratio of the relative effects of the convective (Couette) to diffusive (Poiseuille) terms, analogous to a Peclet number. For applications of interest, small gap heights, small aspect ratios and high speeds all point to large bearing numbers; hence we define $\delta = 1/\Lambda$ as a small parameter.

To complete the formulation of the model, we need to specify a relation between the pressure and the gas density. The simplest choice for the equation of state is the ideal gas law, which states that the pressure is proportional to the product of the density with the temperature. Assuming the temperature to be held fixed, this gives $\rho = kp$ and reduces the Reynolds equation to a PDE for the evolution of the product $p(x,t)h(x,t)$,

$$\frac{\partial(ph)}{\partial t} + \tfrac{1}{2}\frac{\partial(ph)}{\partial x} = \delta\frac{\partial}{\partial x}\left(ph^3\frac{\partial p}{\partial x}\right), \tag{12.24a}$$

on the domain $0 \le x \le 1$ and is subject to the boundary conditions on the pressure,

$$p(0,t) = 1, \qquad p(1,t) = 1. \tag{12.24b}$$

For $\delta \to 0$, this is a singularly perturbed boundary value problem and can be shown to generate a boundary layer in the pressure at $x_* = 1$, the trailing edge of the slider. On the rest of the domain, $0 \le x < 1$, we can approximate the solution by the solution of the leading order outer problem,

$$\frac{\partial(p_0 h)}{\partial t} + \tfrac{1}{2}\frac{\partial(p_0 h)}{\partial x} = 0. \tag{12.25}$$

This is a linear advection equation and yields the solution as a traveling wave with speed one half, $F(x - \frac{1}{2}t)$, which can also be expressed as

$$p_0(x,t)h(x,t) = f(t-2x), \tag{12.26}$$

for some choice of function $f(s)$. Applying the boundary condition on the pressure at $x = 0$ and evaluating the gap height there, from (12.19), $h(0,t) = a(t)$, and we determine $f(t) \equiv a(t)$. Consequently the solution of this signaling-type wave problem for the pressure can be expressed as

$$p_0(x,t) = \frac{a(t-2x)}{a(t)+s(x)}, \tag{12.27}$$

from $p_0 = f/h$. We can now use this representation of the pressure to return to the primary question of the stability and dynamics of the slider.

The motion of the slider is characterized by the height of the leading edge, $y = a(t)$, hence we seek an evolution equation for $a(t)$. This will be provided by a force balance in the vertical direction. As described above, the air flow generates a lift force on the slider, this is given by the integral of the excess pressure over the domain of the slider,

$$F_L(t) = \int_0^1 (p(x,t)-1)\,dx.$$

This balances against the downward applied load imposed on the slider by structural constraints, F_S to yield the force balance equation

$$m\frac{d^2a}{dt^2} = \int_0^1 \frac{a(t-2x)}{a(t)+s(x)}\,dx - (F_S+1), \tag{12.28}$$

where m is the scaled mass of the slider. We note that by neglecting the trailing edge boundary layer in the pressure, we only make a small error, $O(\Lambda^{-1})$ in calculating the lift integral.

We can obtain a time-independent steady-state, $a = \bar{a}$, by solving an algebraic equation,

$$\bar{a}\int_0^1 \frac{dx}{\bar{a}+s(x)} = F_S + 1.$$

Then, we can examine the linear stability of this steady solution to small deviations by assuming a perturbed solution, $a(t) = \bar{a} + \sigma e^{\lambda t}$, for $\sigma \to 0$. Substituting this form into (12.28) yields an equation for the exponential growth rate λ at $O(\sigma)$,

$$m\lambda^2 = \int_0^1 \frac{e^{-2\lambda x}}{\bar{a}+s(x)}\,dx - \int_0^1 \frac{\bar{a}}{(\bar{a}+s(x))^2}\,dx. \tag{12.29}$$

If the governing equation for $a(t)$ were an autonomous ODE, then λ would be given by the roots of a characteristic polynomial. However due to the unusual shifted depen-

dence on the solution in the integral, (12.28) can be related to a delay-differential equation and yields a more challenging transcendental equation for the linear stability analysis. Careful consideration of this problem was explored in [109].

12.3 Rivulets in a Wedge Geometry

In the previous section, we considered a scenario where the substrate was uniformly flat. Here, we investigate a lubrication-type problem for a rivulet (slender thread) of viscous fluid constrained within a wedge geometry[3] (see Fig. 12.3). In particular, we will study the so-called *large-time* dynamics of the problem using asymptotic approximations and self-similar solutions. As well as being a well-observed physical phenomena, interesting in its own right, the results that we obtain also have application to the study of foam drainage, where the flow takes place within the "triangular" shaped region of the Plateau borders[4] (see [103] for a general discussion of the dynamics of foams).

We shall take X to represent the distance along the wedge, with Y as the vertical upward distance from the base of the wedge, and Z as the transverse distance from the centreline of the wedge (along with the respective velocities U, V and W).

We begin with the dimensional Navier-Stokes equations in three-dimensions (12.2); the dimensional density $\tilde{\rho}$ is taken to be constant. We apply the nondimensionalisation

$$\mathsf{X} = \bar{\mathrm{L}}x, \qquad \mathsf{Y} = \bar{\mathrm{H}}y, \qquad \mathsf{Z} = \bar{\mathrm{H}}z, \qquad \mathsf{T} = \bar{\mathrm{T}}t, \tag{12.30a}$$

$$\mathsf{U} = \bar{\mathrm{V}}u/\varepsilon, \qquad \mathsf{V} = \bar{\mathrm{V}}v, \qquad \mathsf{W} = \bar{\mathrm{V}}w, \qquad \mathsf{P} = \bar{\mathrm{P}}p, \tag{12.30b}$$

where $\bar{\mathrm{H}}$ is a typical fluid depth and $\bar{\mathrm{V}} = \varepsilon^2\gamma/\mu$ is a representative velocity scale (here, γ is the coefficient of surface tension for the free surface of the liquid). The expressions (12.30) imply that we consider the magnitude of the flows in the vertical and transverse directions to be of the same order, and (as in the previous section) the aspect ratio $\varepsilon = \mathrm{H}/\mathrm{L} \ll 1$. After substitution and collecting terms in orders of ε, the leading order equations are found to be

$$\frac{\partial p}{\partial x} = \frac{\partial^2 u}{\partial y^2} + \frac{\partial^2 u}{\partial z^2}, \qquad \frac{\partial p}{\partial y} = 0, \qquad \frac{\partial p}{\partial z} = 0, \tag{12.31}$$

being a reduced version of the Stokes equations (12.9). The last two equations of (12.31) show that to leading order the pressure field is independent of both y and z, and hence $p = P(x,t)$. Furthermore, geometric considerations can be used to show

[3] This analysis is based on the paper [16] to which we refer the interested reader for more details.

[4] The sides of a Plateau border are actually circular arcs and there is no free-surface, but the model equations that we derive here are still applicable. This is an example of how modelling and investigating one problem can also provide useful information for other related problems.

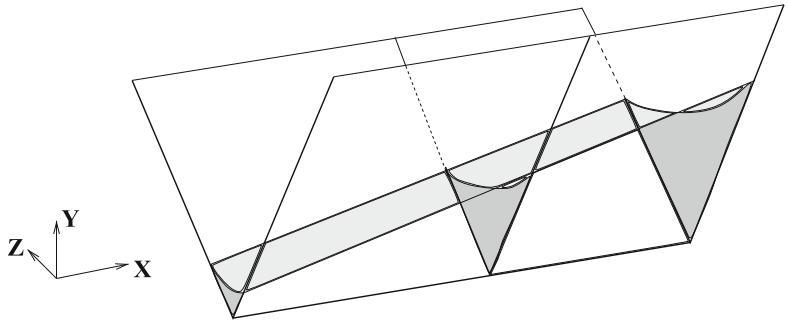

Fig. 12.3 Schematic of the problem geometry

that $P \propto A^{-1/2}$, where $A(x,t)$ is the cross-sectional area of the rivulet at location x and time t. The first equation of (12.31) can be solved subject to no-slip boundary conditions on the substrate and pressure jump conditions across the free surface of the liquid to yield $u \propto A^2 \partial P/\partial x$.

The conservation of mass result for the cross-sectional area $A(x,t)$ takes the form

$$\frac{\partial A}{\partial t} + \frac{\partial}{\partial z}\left(\int_D u\, dy\, dz\right) = 0, \tag{12.32}$$

where D is the area of the (y,z) plane occupied by liquid at fixed x and t. Substituting in the relevant expressions for u and P from above consequently results in a PDE for the evolution of $A(x,t)$ which takes the (porous-medium-equation-type) form

$$\frac{\partial A}{\partial t} = \frac{\partial}{\partial x}\left(A^{1/2}\frac{\partial A}{\partial x}\right), \quad 0 \le x < \infty \tag{12.33}$$

and is the basic equation that we will further analyse. For initial data, we impose

$$A(x,0) = \begin{cases} M & 0 \le x < 1, \\ 0 & x \ge 1, \end{cases} \tag{12.34}$$

corresponding to a constant cross-section of fluid over $0 \le x < 1$ with a dry wedge for $x > 1$; the initial volume of liquid is consequently also given by M.

Once the liquid is in motion ($t > 0$), there will be a moving free-boundary $x = s(t)$ (with $A \equiv 0$ for $x > s(t)$), on which we impose the physically sensible conditions $A = 0$ (zero height) and $A^{1/2}A_x = 0$ (zero flux across the interface). At $x = 0$, we also impose zero flux (corresponding to a solid wall), so that the total mass of liquid in the wedge is conserved for all time, i.e.

$$\frac{d}{dt}\int_0^{s(t)} A(x,t)\,dx = 0 \quad \Longrightarrow \quad \int_0^{s(t)} A(x,t)\,dx = \int_0^{s(t)} A(x,0)\,dx = M. \tag{12.35}$$

The nonlinear diffusion equation (12.33) coupled with the conservation law (12.35) admits a similarity solution

$$A = t^{-2/5} f(\eta), \quad \eta = \frac{x}{t^{2/5}}, \tag{12.36}$$

where $f(\eta)$ satisfies

$$-\frac{2}{5}\left(f + \eta \frac{df}{d\eta}\right) = \frac{d}{d\eta}\left(f^{1/2}\frac{df}{d\eta}\right),$$

with solution

$$f(\eta) = \frac{1}{100}(\eta_0^2 - \eta^2)_+^2; \tag{12.37}$$

the subscripted plus sign here denotes that we are only interested in the non-negative part of the solution, with the moving interface $x = s(t)$ corresponding to $\eta = \eta_0$ in terms of the similarity variables. Of course, (12.36) is singular in the limit $t \to 0^+$ and so cannot satisfy the initial condition (12.35). However, it is well-known that similarity solutions often act as large-time attractors for the dynamics of nonlinear diffusion equations and so we can expect $A(x,t)$ to approach (12.36) and (12.37) at large times.

12.3.1 Imbibition in a Vertical Wedge

Suppose now that we orient the wedge so that it is vertical, with the base located at $x = 0$. In such a geometry, we can no longer neglect gravity and it will be the competing effects of gravity (acting downwards) and capillarity (acting upwards) that drives the motion of the fluid.

Taking gravity to act equally everywhere on the fluid leads to a convective flow in the downward direction that requires the evolution Eq. (12.33) to be adjusted to read

$$\frac{\partial A}{\partial t} - 2A\frac{\partial A}{\partial x} = \frac{\partial}{\partial x}\left(A^{1/2}\frac{\partial A}{\partial x}\right), \quad 0 \le x < \infty; \tag{12.38}$$

we note that the left-hand-side terms of (12.38) correspond to a quasilinear convection equation that can be tackled by the method of characteristics (starting from the initial data (12.34)) and shown to have smooth solutions for all $t > 0$.

Physically, we expect the amount of liquid that can be pulled up the wedge by capillarity to be small compared to the bulk mass. We therefore assume that the solution in the latter region will effectively be a steady-state solution of (12.38) and consequently find

$$A = \frac{4}{(x + x_0)^2} \quad \text{for} \quad x = O(1). \tag{12.39}$$

The value of x_0 is set (to leading order) by the mass constraint (12.35), by which we calculate $x_0 = 4/M$. The steady-state *inner solution* (12.39) will match to the *outer solution* governed by capillary action.

In the capillary flow region, we cannot neglect the time-dependence in (12.38). We do not attempt to derive an exact solution of (12.38), but note that it admits a similarity solution of the form

$$A = t^{-2/3} g(\mu), \quad \mu = \frac{x}{t^{1/3}}, \tag{12.40}$$

with $g(\mu)$ satisfying

$$-\frac{2}{3} g - \frac{1}{3} \mu g_\mu = \left(g^{1/2} g_\mu - g^2 \right)_\mu .$$

Close to $x = s(t)$, with $s(t) = \mu_0 t^{1/3}$ in terms of the similarity variables,

$$g \sim \frac{\mu_0^2}{36} (\mu_0 - \mu)^2 \quad \text{as} \quad \mu \to \mu_0^-,$$

so that the solution has zero contact angle at $\mu = \mu_0$. As $\mu \to 0^+$ we must match with (12.39) as $x \to \infty$ and this requires that

$$g \sim \frac{4}{\mu^2} \quad \text{as} \quad \mu \to 0^+.$$

A schematic of the overall (large-time) solution structure is shown in Fig. 12.4.

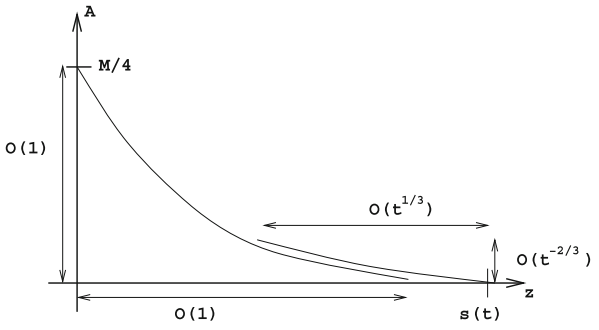

Fig. 12.4 Schematic of the large-time solution for gravity opposing capillarity based on the solution of Eq. (12.38)

12.3.2 Draining in a Vertical Wedge

In this scenario, $x = 0$ is taken to be at the top of the wedge, with the liquid moving downwards (again starting from (12.34)) under the now combined effects of gravity and capillarity. The evolution equation takes the same form as (12.38), except for a different sign on the convective term

$$\frac{\partial A}{\partial t} + 2A\frac{\partial A}{\partial x} = \frac{\partial}{\partial x}\left(A^{1/2}\frac{\partial A}{\partial x}\right), \quad 0 \le x < \infty; \tag{12.41}$$

notably, in contrast to the case of imbibition, the quasilinear equation allows shocks to form and we will observe this phenomena in the large time solution to (12.41).

Away from $x = 0$, the dynamics of the (*outer region*) solution are primarily controlled by the effects of gravity and the reduced PDE is consequently given by

$$\frac{\partial A}{\partial t} \sim -2A\frac{\partial A}{\partial x}, \tag{12.42}$$

with a solution of self-similar form

$$A = t^{-1/2}h(v), \quad v = \frac{x}{t^{1/2}}. \tag{12.43}$$

Here, $h(v)$ satisfies

$$\frac{1}{2}\frac{d}{dv}(hv) = \frac{d}{dv}(h^2),$$

so that

$$h = \begin{cases} \frac{1}{2}v & 0 < v < v_0, \\ 0 & v > v_0. \end{cases} \tag{12.44}$$

Standard matching arguments imply that $A \sim z/2t$ as $v \to 0^+$, while conservation of mass (12.35) determines the shock location $v_0 = 2\sqrt{M}$. Across the shock, the effects of capillarity are important and smooth the solution over a narrow *interior layer* with scalings

$$x = s(t) + t^{1/4}\xi, \quad s \sim v_0 t^{1/2}, \quad A \sim t^{-1/2}\Phi(\xi).$$

As a result, we find

$$\Phi(\xi) = \frac{v_0}{2}\tanh^2\left(\frac{1}{2}\sqrt{\frac{v_0}{2}}\xi\right), \tag{12.45}$$

which corresponds to a travelling wave solution of (12.41).

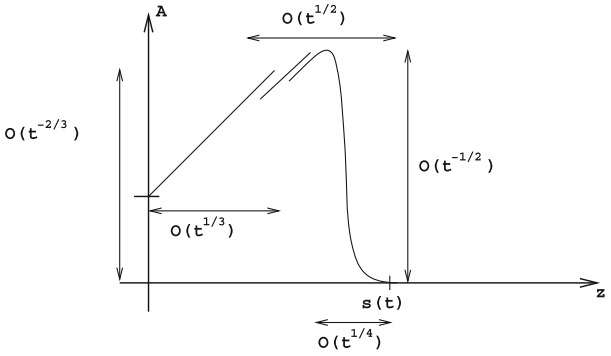

Fig. 12.5 Schematic of the large-time solution for gravity assisting capillarity based on the solution of Eq. (12.41)

The (*inner solution*) behaviour close to $x = 0$ is again given by (12.40), with $g \sim \mu/2$ as $\mu \to \infty$ in order to match with the outer solution. Finally, as $u \to 0^+$, we have $g \sim g_0 + g_0^{3/2} v$ as a consequence of the zero-flux boundary condition imposed at $x = 0$; numerical calculations yield $g_0 \approx 0.5885$. The entire large-time solution structure is illustrated schematically in Fig. 12.5.

A number of extensions of this problem are possible, such as the introduction of an influx of liquid at $x = 0$ and the investigation of different geometries for the wedge shape (see [16] for a detailed description of the previous analysis and further extensions).